ROYAL SOCIETY OF CHEMISTRY

PAPER

Check for updates

Acoustic separation of living and dead cells using high density medium†

Karl Olofsson, [iD] Björn Hammarström [iD] and Martin Wiklund [iD] *

The acoustic radiation force, originating from ultrasonic standing waves and utilized in numerous cell oriented acoustofluidic applications, is dependent on the acoustic contrast factor which describes the relationship between the acousto-mechanical properties of a particle and its surrounding medium. The acousto-mechanical properties of a cell population are known to be heterogeneously distributed but are often assumed to be constant over time. In this paper, we use microchannel acoustophoresis to show that the cell state within a cell population, in our case living and dead cells, influences the mechanical phenotype. By investigating the trapping location of viable and dead K562, MCF-7 and A498 cells as a function of the suspension medium density, we observed that beyond a specific medium density the viable cells were driven to the pressure anti-node while the dead cells were retained in the pressure node. Using this information, we were able to calculate the effective acoustic impedance of viable K562 and MCF-7 cells. The spatial separation between viable and dead cells along the channel width demonstrates a novel acoustophoresis approach for binary separation of viable and dead cells in a cell-size independent and robust manner.

Introduction

Microfluidic methods for separation, spatial control and analysis of cells are appreciated for their potential to substantially reduce time and reagents needed in clinical settings and basic biology research.[1] One approach to gently and non-invasively manipulate the position of cells and particles is acoustophoresis[2] which has been extensively used in concentration,[3] washing,[4] separation,[5] trapping[6,7] and acoustic streaming[8,9] applications. The acoustophoresis principle in bulk acoustic wave applications is based on establishing an acoustic standing wave in a fluid containing cavity such as a microfluidic channel,[10] chamber[11,12] or well.[13] Due to non-linear scattering of the acoustic wave, the stationary pressure field exert acoustic radiation forces on small particles or cells suspended in the fluid filled cavity.[14] These acoustic radiation forces and pressure fields have been proven safe for cells in several studies.[15,16]

The acoustic radiation force magnitude depends on several factors such as frequency, acoustic energy density, particle volume and the acoustic contrast factor Φ_{ac} which describes the relationship between the density and compressibility of the suspended cells and the surrounding

fluid. In a standing wave, the sign of the acoustic contrast factor Φ_{ac} is important for controlling whether a suspended particle is driven to the pressure node or anti-node. This can be utilized in separation techniques involving *e.g.* antibody coated microbubbles[17] for specific and binary separations. Binary separations based on the acoustic contrast factor are in general less sensitive to the balance between flow rate and acoustic energy density in the microchannel.

While most acoustophoretic separation methods take advantage of the strong particle/cell volume dependence in the acoustic radiation force, a recent publication by Augustsson *et al.*[18] presents a new separation and acousto-mechanical phenotyping technique based on introducing a fluid density gradient across the channel width. This technique shows the importance of acousto-mechanical cell properties and the advantages of size independent separation. For the continued progress of acoustophoretic separation techniques, both cell volume- and acousto-mechanical based, it is vital to know the mechanical properties of cell populations. The mechanical properties of cells have been shown through acoustic microscopy,[19,20] with sub-cellular resolution, to depend on intracellular organization and have been measured in bulk[21] and on single cells[22–25] through different techniques.

While these studies and measurement methods provide great insight to the mechanical state of cells it is often assumed that the mechanical properties of a cell are, although distributed heterogeneously over a cell population, constant. In this study we show that the acousto-mechanical

---

Department of Applied Physics, KTH Royal Institute of Technology, Sweden.
E-mail: martin.wiklund@biox.kth.se

properties of cells are dynamic features that depend on cell state which can affect acoustophoresis applications and introduce systematic errors if cells are affected before analysis and might impact *e.g.* separation efficiency. We highlight the dynamic characteristics of the acousto-mechanical properties by studying the influence of medium density on the acoustic contrast factor Φ_{ac} using the case of living and dead human K562 leukemia cells, MCF-7 breast cancer cells and A498 renal carcinoma cells. In cell suspensions containing viable and dead cells, we added a density modifying molecule (iodixanol) at several concentrations ranging from 0% to 30% v/v and studied the mixed cell populations during acoustophoresis in a straight channel. We found that the acoustic contrast factor sign for viable K562 and MCF-7 cells change from positive to negative by observing a shift in trapping position, from pressure node to pressure anti-node, at iodixanol concentrations over 20%. Fixed K562 and MCF-7 cells remained in the pressure node over the whole concentration range, as a result of the acoustic contract factor being a function of the cell membrane permeability. We also used the ratios of viable K562 and MCF-7 cells in the pressure node, anti-node and the intermediate positions over the whole concentration range to approximate the effective acoustic impedance to Z_{K562} = 1.68 ± 0.014 MPa s m^{-1} and Z_{MCF-7} = 1.67 ± 0.012 MPa s m^{-1}. The separation method was confirmed by measuring a high acoustic separation efficiency between viable and starved or osmotic shock treated K562, MCF-7 and A498 cells suspended in 30% v/v iodixanol concentration. This work does not only show the importance of cellular state in acoustophoresis applications but also provides a cell-size independent method to binary sort cell populations based on cell viability.

Theory

Consider a small particle with radius a, density ρ_c and compressibility κ_c suspended in a liquid with density ρ_0 and compressibility κ_0. If a pressure and velocity field is present, the small particle will experience an acoustic radiation force F_{rad} which in case of a standing wave in 1-D along the z-axis can be described by the expression[14]

$$F_{rad} = 4\pi\Phi_{ac}(\tilde{\kappa},\tilde{\rho})ka^3E_{ac}\sin^2(2kz) \tag{1}$$

where k is the wavenumber. The compressibility ratio $\tilde{\kappa}$ and density ratio $\tilde{\rho}$ are explained further down when defining the acoustic contrast factor Φ_{ac}. The acoustic energy density E_{ac} for a pressure field amplitude p_a is defined as

$$E_{ac} = \frac{p_a{}^2}{4\rho_0 c_0{}^2}. \tag{2}$$

Relevant in this study is the acoustic contrast factor Φ_{ac} which describes the relationship between the density and compressibility of the small particle and the wave carrying fluid. Depending on this relationship, Φ_{ac} can be both positive and negative and decides the acoustic radiation force

direction as well as whether the particle is driven to the pressure node ($\Phi_{ac} > 0$) or pressure anti-node ($\Phi_{ac} < 0$). The acoustic contrast factor is expressed through the acoustic monopole and dipole scattering coefficients, $f_1(\tilde{\kappa})$ and $f_2(\tilde{\rho})$, defined as:

$$\Phi_{ac}(\tilde{\kappa},\tilde{\rho}) = \frac{1}{3}f_1(\tilde{\kappa}) + \frac{1}{2}f_2(\tilde{\rho}) \tag{3}$$

where the acoustic monopole and dipole scattering coefficients are given by

$$f_1(\tilde{\kappa}) = 1 - \tilde{\kappa}, \tag{4}$$

$$f_2(\tilde{\rho}) = \frac{2(\tilde{\rho}-1)}{2\tilde{\rho}+1}. \tag{5}$$

The acoustic monopole scattering coefficient $f_1(\tilde{\kappa})$ depends on the particle/fluid compressibility ratio $\tilde{\kappa} = \kappa_c/\kappa_0$ and the acoustic dipole scattering coefficient $f_2(\tilde{\rho})$ is a function of the particle/fluid density ratio $\tilde{\rho} = \rho_c/\rho_0$.

Methods

Cell culture and staining

In this study we used human K562 leukemia cell line (K562 ATCC CCL-243™), human MCF-7 breast cancer cell line (gift from Fernandez-Capetillo lab, cell line identity confirmed using short-tandem repeat profiling analysis by ATCC) and human A498 renal carcinoma cell line (A498 ATCC HTB-44™). K562 is a suspension cell line while MCF-7 and A498 are adherent cell lines. K562 and A498 were cultured in T25 flasks and suspended in complete cell medium consisting of HyClone™ RPMI-1640 (GE Healthcare) supplemented with 10% fetal bovine serum (FBS) (GE Healthcare) and 100 U mL^{-1} penicillin–100 mg mL^{-1} streptomycin while MCF-7 were suspended in HyClone™ DMEM (GE Healthcare) supplemented like the RPMI-1640 complete medium. Cells were maintained by splitting every second day.

Two fluorescent dyes were used to distinguish viable and fixed/dead cells in the microscopy images; cell-permeant CellTrace calcein red-orange (RO) AM (Invitrogen) for living cells and cell-impermeant SYTOX Blue (Invitrogen) for dead cells. Living cells were prepared for staining by washing in PBS and centrifuging (1600 RPM for 5 minutes) two times. The supernatant was discarded and the cells were incubated in 37 °C for 10 minutes in PBS with 1 μM calcein RO. After two centrifugal washing steps with complete cell medium the stained cells were resuspended to a final concentration of 1.2 × 10^6 cells per mL.

To model dead cells, fixed and permeabilized K562 and MCF-7 cells were prepared by washing and centrifuging cells in PBS before being resuspended in BD Cytofix/Cytoperm™ solution (BD Biosciences) containing 4% paraformaldehyde (PFA) and incubated protected from light for 10 minutes in room temperature. The fixed cells were washed and stained in PBS containing 1 μM SYTOX Blue for 10 minutes in room temperature before two centrifugal washes in complete

medium. Stained and fixed cells were resuspended to a final concentration of 1.2×10^6 cells per mL.

Two death conditions, osmotic shock and starvation, were triggered on K562, MCF-7 and A498. Cell death by osmotic shock was induced by adding 10X PBS for 24 hours prior to the experiment. MCF-7 and A498 were incubated with 10X PBS in their adherent state while K562 was centrifuged and resuspended with 10X PBS. 10X PBS contains 10 times the salt concentration which exerts a high osmotic pressure on the cells. Cell death by starvation was induced by maintaining the cells in PBS instead of complete medium for 72 hours prior to staining and separation. In both cases, cell death was confirmed by Trypan blue before staining and sample preparation.

### Density modulated media sample preparation

Adjusting the suspension medium density allows for investigations of how the acoustic contrast factor Φ_{ac} of cells is influenced by the mechanical properties of the wave carrying fluid. We have used the density gradient medium OptiPrep™ (STEMCELL Technologies, Norway) containing 60% v/v iodixanol in this work which has been used in previous studies investigating the acousto-mechanical properties of cells.[18]

Solutions with 0%, 10%, 15%, 20% 25% and 30% v/v iodixanol in complete cell medium was used to mix and suspend calcein RO stained living cells and SYTOX Blue stained fixed cells to a final cell concentration of 6×10^5 cells per mL (living cells: 3×10^5 cells per mL, dead cells: 3×10^5 cells per mL). The density modified cell suspensions were sequentially investigated and images captured in a microscope when acoustic radiation forces acted on the cells. Only the 30% v/v iodixanol concentration condition was tested for the starvation and osmotic shock treated K562, MCF-7 and A498 cells.

Ultrasonic device setup and operation

The device used in this study consists of a silicon and glass microfluidic chip (GeSiM GmbH, Germany) (Fig. 1A-1) with four inlet/outlets connected to a straight channel. Only one inlet (Fig. 1A-2) and one outlet (Fig. 1A-3) were used with plastic tubing connected to syringes and connected to the chip through O$_2$ plasma bonded PDMS gaskets (Fig. 1A-4). The unused inlets/outlets were sealed with Kapton tape (Fig. 1A-5). A piezoelectric transducer, with a 2 MHz resonance in thickness mode, was glued to the top of the chip (Fig. 1A-6) to generate acoustic waves through an electric sinusoidal signal carried by conducting wires soldered to the piezo electrodes (Fig. 1A-7) and connected to a signal generator and amplifier. An oscilloscope was used to measure the voltage over the piezo electrodes.

The microfluidic chip consists of a 110 μm thick silicon wafer with a straight 375 μm wide channel etched straight through and sealed with a 170 μm glass bottom and 1000 μm thick glass top in a sandwich construction (Fig. 1B). During
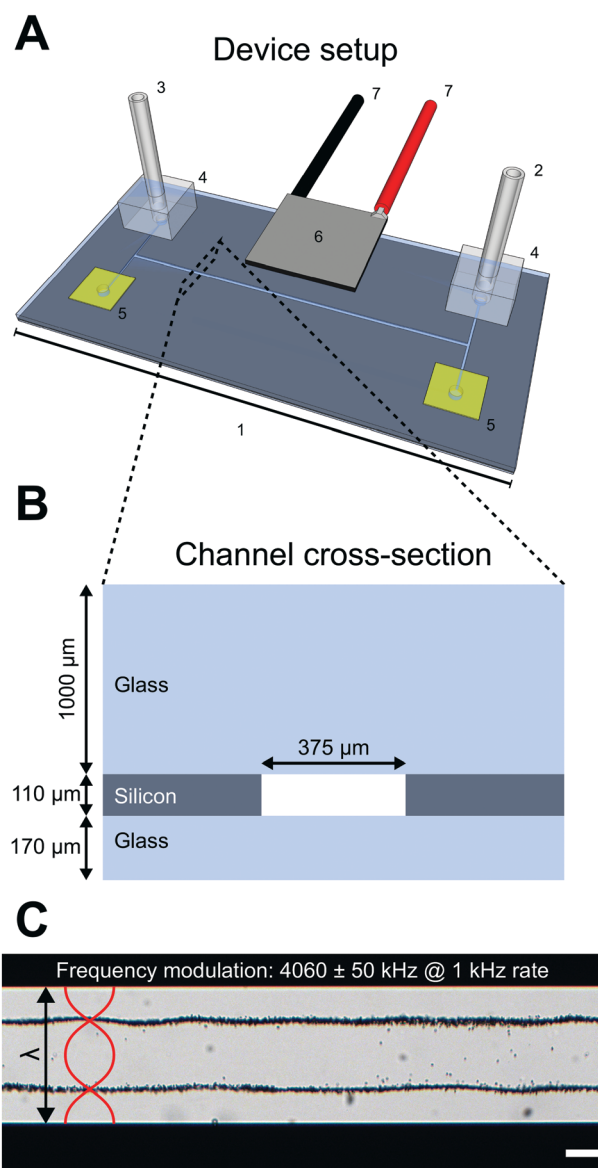
Fig. 1 Device overview. The device consists of a glass/silicon microfluidic chip (1) with four exits where fluid carrying tubing is connected to the inlet (2) and outlet (3) with through O$_2$ plasma bonded PDMS connectors (4). The unused channel exits were blocked by Kapton tape (5). A piezoceramic element (6) glued to the microfluidic top was used to introduce ultrasonic waves into the chip by actuating the piezo with electric sinusoidal signals carried through wires soldered to the electrodes (7) (A). The microfluidic chip is a glass/silicon/glass sandwich construction where the channel geometry is etched straight through a 110 μm silicon wafer before being bonded to a 170 μm and 1000 μm glass wafer. The channel width is 375 μm (B). When the piezo ceramic element is excited by a frequency matching the full wavelength (λ) criterion, a standing wave is established in the channel and particles suspended in the channel liquid is subjected to ultrasonic radiation forces. An example is shown in (C) where 5 μm polystyrene beads suspended in water, without any density modifying molecules, were trapped in the two pressure nodes when a frequency modulation scheme was applied to the piezo (4060 ± 50 kHz at 1 kHz rate). Scalebar is 100 μm.

experiments with cells and beads the piezoelectric transducer was excited around the second harmonic frequency 4.06 MHz which corresponds to a full wavelength across the microfluidic channel width. A frequency modulation scheme, where the frequency of the sinusoidal signal was swept linearly at 1 kHz in a sawtooth fashion over a 100 kHz span around the center frequency 4060 kHz, was used to robustly meet the λ criterion when different density adjusted cell suspensions were introduced into the channel. The excitation voltage across the piezo electrodes was 8.2 Vpp.

The pressure and velocity fields, with two pressure nodes situated $\lambda/4$ from each channel wall and three pressure anti-nodes (one in the channel center and one by each channel wall), exert acoustic radiation forces on small particles. Depending on the acoustic contrast factor Φ_{ac}, the particles will either be forced into the pressure node or anti-node. As an example, 5 μm polystyrene beads suspended in MilliQ water with 0.1% Tween-20 have a positive acoustic contrast factor and will be forced into the two pressure nodes when the piezo transducer is actuated as stated above (Fig. 1C).

Microscopy and imaging

All experiments and data acquisition in this study was performed using an inverted microscope (Axiovert 40 CL, Zeiss, Germany) equipped with a mercury lamp for fluorescent excitation and a long working distance objective (LMPlanFL 20×/0.40, Olympus, Japan). A 5-megapixel C-mount equipped RGB USB-3 camera (BlackFly S Color Sony IMX250, FLIR, OR, USA) controlled by an inhouse developed LabView script was used for image acquisition. During cell experiments which involved the two differently stained cell populations, both fluorescent excitation and regular transmission microscopy was employed to allow cell classification and cell position measurement in the channel during stop-flow conditions.

Results

### Acoustic separation of viable and fixed cells

To investigate the influence of cell state on the acousto-mechanical properties, the acoustophoretic motion of living and dead K562 cells suspended in a high-density medium was compared to that of cells suspended in a regular medium (Fig. 2). Living cells (Fig. 2B) were identified by their morphology and orange color (calcein RO), whereas fixed and dead cells (Fig. 2C) were identified by their blue color (SYTOX blue). When the piezoelectric transducer was actuated with the frequency modulation scheme (4060 ± 50 kHz @ 1 kHz rate) at 8.2 Vpp over the piezo electrodes while no density modifying iodixanol was present in the cell suspension, both living and fixed cells were trapped in the pressure node (Fig. 2D). However, when living and dead cells were suspended in medium containing 25% v/v iodixanol, viable cells were manipulated into the pressure anti-node, implying a negative acoustic contrast factor Φ_{ac}, while the dead cells were still forced into the pressure node (Fig. 2E).

Quantification of separation efficiency between live and fixed cells

To quantify the phenomena where living and fixed cells can be separated using ultrasonic standing waves and a density modified medium, cell suspensions with a series of iodixanol concentrations (0%, 10%, 15%, 20%, 25% and 30% v/v) were introduced into the microfluidic channel during piezo actuation. Under the influence of acoustic radiation forces, positions of viable and fixed K562 and MCF-7 cells were recorded in micrographs for each iodixanol concentration. New cells were introduced into the microscope camera field of view before each image acquisition under stop-flow conditions. To reduce the influence of inhomogeneous cell volume on the final cell position in the channel, cells were allowed to be manipulated by acoustic radiation forces for a couple of
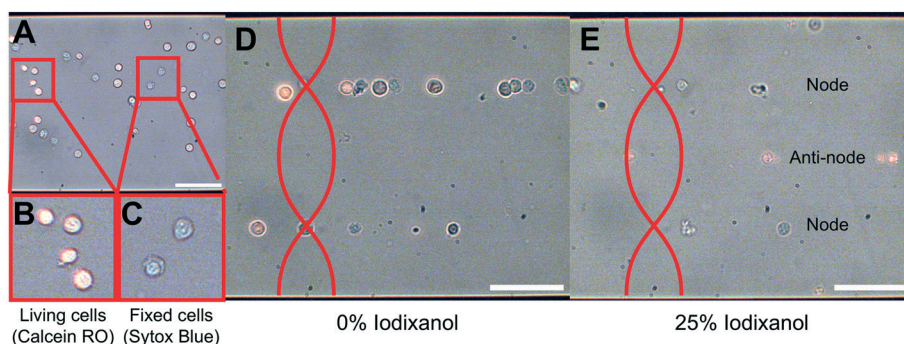
Fig. 2 The acoustic contrast factor Φ_{ac} of living and dead cells has opposite signs in high-density medium. A suspension of living K562 cells labeled with calcein red-orange and SYTOX Blue labeled fixed K562 cells were introduced into the microfluidic channel (A). Through simultaneous fluorescence excitation and transmission imaging it was possible to distinguish living (B) and fixed (C) cells. No ultrasonic actuation was present in (A)–(C). When living and dead cells were influenced by ultrasonic radiation forces in regular cell medium, both populations had a positive acoustic contrast factor Φ_{ac} and were manipulated into the pressure node (D). If the cells were suspended in a high-density solution containing 25% v/v iodixanol, the acoustic contrast factor Φ_{ac} for the living cells was negative and living cells were forced to the pressure anti-node while fixed cells with compromised cell membrane still had a positive acoustic contrast factor and were manipulated into the pressure node (E). All scale bars are 100 μm.
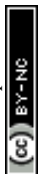
seconds before an image was captured. Medium density in high iodixanol concentrations made especially living cells buoyant and the objective focus was adjusted to account for this to reduce bias in the data. Fixed/dead cells were less affected by buoyancy effects and could be predominantly be found at close to the channel bottom at all concentration levels.

From the micrographs, data based on the cell position along the standing wave propagation axis within the microchannel was quantified. Each image was divided into zones corresponding to pressure node (blue), pressure anti-node (red) and intermediate areas between the node and anti-node (cyan) (Fig. 3A). The width of the pressure node and central pressure anti-node zones was chosen to be approximately twice the K562 cell diameter ($d_{K562} \sim 10$ μm) while the two pressure anti-node zones adjacent to the microchannel walls had a width of single K562 cell diameter. The wider zone width for the central anti-node and the two nodes was chosen to accommodate slight changes in acoustic pressure field contour along the channel length. With these zones specified, cells in 15 micrographs from each iodixanol concentration condition was manually classified as living or dead and placed in either zone. Distributed over the whole concentration range, 455 living K562 cells, 524 fixed K562 cells, 429 viable MCF-7 cells and 648 fixed MCF-7 cells were counted, classified and positioned. Out of focus cells were discarded from the analysis but micrographs acquired with objective focus close to the bottom and top were both included in the analysis for iodixanol concentrations where viable and dead or fixed cells were situated at different channel heights.

At low iodixanol concentrations (0–15%), living K562 cells had a positive acoustic contrast factor and were trapped in the pressure node while a transition point where the acoustic contrast factor sign changes was reached at 20% v/v iodixanol concentration. At this iodixanol concentration the largest number of cells (≈48%) were found in the intermediate zone, indicating no acoustic contrast between the fluid and the cell ($\Phi_{ac} = 0$), while some cells were still found in the pressure node (≈43%) and anti-node (≈9%). At and above 25% v/v iodixanol concentration, a majority of viable cells were found in the pressure anti-node (Fig. 3B). Viable MCF-7 cells followed a similar trapping pattern as K562 over the iodixanol concentration range but required a lower iodixanol concentration for a displacing all cells into the pressure anti-node (25%) (ESI† Fig. S1A). Fixed K562 and MCF-7 cells characterized, placed and counted from the same set of images as the viable cells, were instead found almost entirely in the pressure node across all investigated iodixanol concentrations (Fig. 3C, ESI† Fig. S1B). Common for both cell lines was that viable cells with zero acoustic contrast factor was affected by streaming and that cell velocities induced by the acoustic radiation force was lower with higher iodixanol concentrations (data not shown).

Acoustic impedance of living K562 and MCF-7 cells

To better predict at which iodixanol concentration the acoustic contrast factor of living cells change sign from
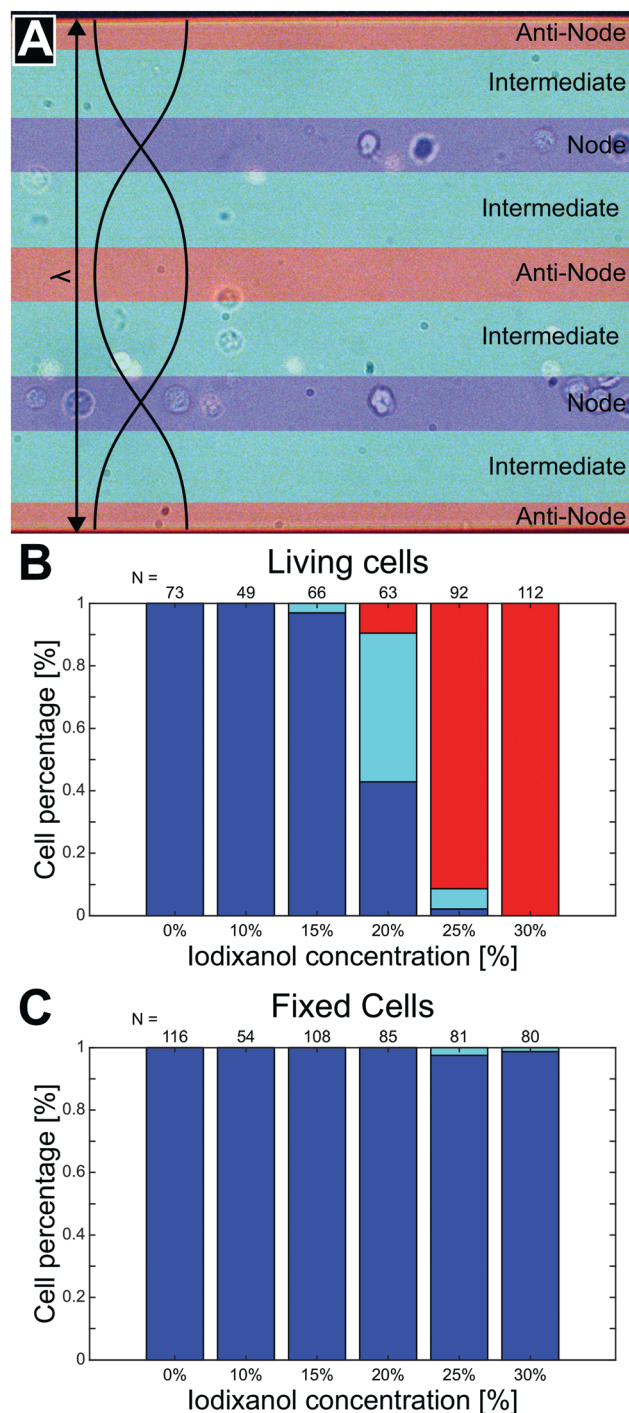
Fig. 3 The separation efficiency of living and fixed K562 cells depends on iodixanol concentration. To quantify the separation efficiency of living and dead cells using a density modified solution, microscopy images of trapped cells captured under stop-flow conditions were divided into three zones; pressure node (blue), pressure anti-node (red) and intermediate (cyan) (A). Cells were manually classified as living or dead depending on fluorescence and placed in either of the three zones. The graphs show the percentage of living (B) and fixed (C) K562 cells found in each zone. The number N of viable and fixed cells characterized and positioned for each concentration condition is found above each histogram bar.

positive to negative we took advantage of the data in Fig. 3B and ESI† Fig. S1A to calculate the effective acoustic impedance of viable K562 and MCF-7 cells. At 20% v/v iodixanol the viable cell populations exhibited zero, positive, and negative acoustic contrast factor. Therefore, we can conclude that the acoustic properties are not homogenous but distributed. This inhomogeneity was assumed to be normally distributed and we used the mean μ and standard deviation σ as fitting parameters. We also introduced a fitting parameter a to account for the cell ratio in the intermediate zone which skews the data along the concentration axis. These parameters were used to simultaneously fit the cumulative distribution function (CDF) of a normal distribution against the ratio of viable K562 and MCF-7 cells in the pressure node (blue line, $y = 1 - \mathrm{cdf}(c_{\mathrm{Iodixanol}} - a, \mu, \sigma)$) and in the pressure anti-node (red line, $y = \mathrm{cdf}(c_{\mathrm{Iodixanol}} + a, \mu, \sigma)$). For K562 the mean was $\mu_{\mathrm{K562, Iodixanol}} = 21.05\%$ (dashed black line), standard deviation $\sigma_{\mathrm{K562, Iodixanol}} = 1.90\%$ and $a_{\mathrm{K562}} = 1.4$ (Fig. 4A). The MCF-7 fit resulted in the mean $\mu_{\mathrm{MCF-7, Iodixanol}} = 20.56\%$, standard deviation $\sigma_{\mathrm{MCF-7, Iodixanol}} = 1.63\%$ and $a_{\mathrm{MCF-7}} = 1.16$ (Fig. 4B). The goodness of fit measured as the squared 2-norm of the residual was 9.27×10^{-4} for K562 cells and 0.0127 for MCF-7.

From the rationale in the paper of Augustsson *et al.*[18] we used that the acoustic impedance of cells and the medium is closely approximated as $Z_{\mathrm{cell}} = Z_{\mathrm{medium}}$ when the acoustic contrast factor is zero ($\Phi_{\mathrm{ac}} = 0$). Using the acousto-mechanical measurements of iodixanol solutions over several concentrations from Augustsson *et al.*, the effective acoustic impedance was calculated to $Z_{\mathrm{K562}} = 1.68 \pm 0.014$ MPa s m^{-1} and $Z_{\mathrm{MCF-7}} = 1.67 \pm 0.012$ MPa s m^{-1} (mean ± standard deviation).

Separation of living and dead cells

Two death conditions, osmotic shock and starvation, were induced on K562, MCF-7 and A498 to test the acoustic separation method without the potential influence of PFA fixation on the cell acousto-mechanical properties. Mixed live and dead cell suspensions containing 30% v/v iodixanol were treated and analyzed under the same conditions as the viable and fixed cell suspensions. Viable and dead cells were identified by fluorescent signal and morphology. Cell death triggered by starvation in all cell lines and the osmotic shock treated K562 cells resulted in a negligible change in shape and cell size compared to their viable state (data not shown). The osmotic shock treatment induced a lamella shaped morphological change in the two adherent cell lines, MCF-7 and A498, compared to their viable, trypsinized and suspended counterpart (ESI† Fig. S2).

At 30% iodixanol concentration, dead K562 and MCF-7 cells through starvation and osmotic shock were efficiently separated (Fig. 5A and B) with only a couple cells being found in the intermediate zones. The separation efficiency of viable and dead cells for A498 cells were affected to a larger degree by dead cells found in the intermediate zones (starved A498 $\approx 13\%$ and osmotic shock treated A498 $\approx 9\%$). The acoustic

$Z_{\mathrm{K562}}= 1.68 \pm 0.014$ MPa•s/m

$Z_{\mathrm{MCF-7}} = 1.67 \pm 0.012$ MPa•s/m
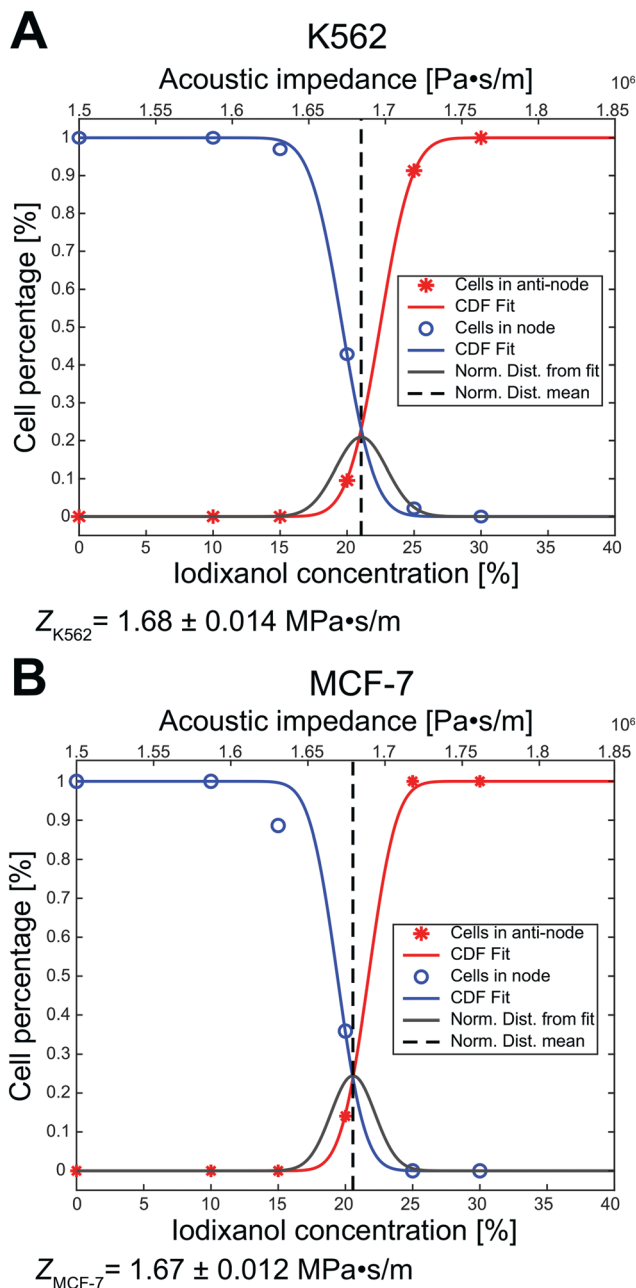
Fig. 4 The acousto-mechanical properties of living K562 and MCF-7 can be estimated using the acoustic contrast sign change. By fitting the cumulative distribution function (CDF) of a normal distribution (squared-2 norm of the residual = 9.27×10^{-4} for K562 and 0.0127 for MCF-7) to the ratio of living cells in the pressure node (blue) and anti-node (red) against iodixanol concentration, the transition point where the acoustic contrast factor change sign for K562 (A) and MCF-7 (B) cells was found. The mean acoustic impedance of viable K562 cells was calculated to be 1.68 ± 0.014 MPa s m^{-1} (mean ± standard deviation) and 1.67 ± 0.012 MPa s m^{-1} for viable MCF-7 cells. The dark grey line represents the normal distribution acquired from the mean μ and standard deviation σ.

contrast factor of viable cells were negative for all cell lines when suspended in 30% v/v iodixanol medium. A general observation for both starved and osmotic shock treated K562 and MCF-7 cells was a slightly lower cell displacement velocity compared to the PFA fixed condition.
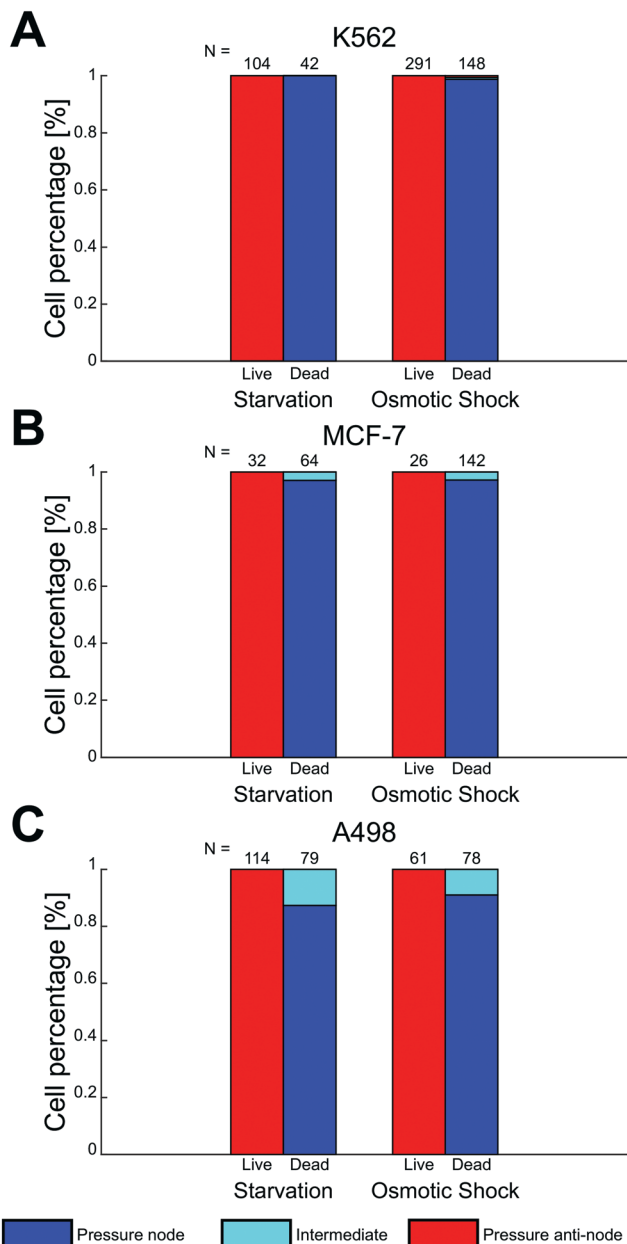
Fig. 5 Cells dead through starvation and osmotic shock were spatially separable from viable cells in 30% v/v iodixanol concentration medium. Mixed suspensions of viable and dead K562 (A), MCF-7 (B) and A498 (C) containing 30 v/v iodixanol were studied under the influence of acoustic radiation force. The final trapping location of cells were in the pressure node (blue), intermediate (cyan) and the pressure anti-node (red) zone. Bar plots show the relative cell count for viable and dead cells in respective zone and the number N above each bar indicates the number of counted cell for each condition.

Discussion

This study shows the importance of cell state in acoustophoresis applications by manipulating the density of the medium in cell suspensions containing living and fixed or dead cells. If the medium density is above a certain level, viable cells are forced into the pressure anti-node since the

acoustic contrast factor of living K562, MCF-7 and A498 cells change sign from positive to negative, while fixed or dead cells stay in the pressure node over the iodixanol concentration range covered in this study. By measuring the ratio of fixed and viable cells in the pressure node, anti-node and the intermediate areas along a straight channel as a function of iodixanol concentration (0–30% v/v), we were also able to find the tipping point were the living K562 and MCF-7 cells have a zero acoustic contrast factor and the acoustic impedance distribution was found.

A shift in acoustic contrast factor sign from positive to negative has previously been shown for living cells suspended in high density medium.[18] The key finding herein is that fixed and dead cells are not driven into the pressure anti-node even at high iodixanol concentrations (Fig. 3C and 5). In a recent publication, Cushing *et al.* presented a method to measure the density and compressibility of cells by measuring the speed of sound in cell suspensions containing a density modifying agent (Percoll) concentration which made cells neutrally-buoyant.[21] They tested both living and fixed cells from several cell lines and systematically found that fixed cells had a lower acoustic contrast factor in PBS compared to their living counterpart which indicates that dead and fixed cells would acquire a negative contrast factor at lower iodixanol concentrations compared to living cells. This could imply that the results in this study are contradicting those reported by Cushing *et al.* However, we propose that dead and fixed cells with a compromised cell membrane, will allow the surrounding liquid to enter the cell and alter the acousto-mechanical properties of a dead cell accordingly. This would make the acousto-mechanical properties of permeabilized cells a function of the surrounding medium and explain the apparent discrepancy between the results in this paper and the Cushing *et al.* study. In this view, the naturally-buoyant cell suspension with fixed cells, reported in the publication by Cushing *et al.*, is an effective way to measure the average density of the organelles and cytoskeleton remaining in the cell. However, the cell density ρ_c, responsible for the acoustic scattering dipole coefficient $f_2(\tilde{\rho})$ in the acoustic contrast factor $\Phi_{ac}(\tilde{\kappa}, \tilde{\rho})$, will depend on the surrounding liquid which immerse the cell through the compromised cell membrane. The same argument can be used for the cell compressibility κ_c in the acoustic scattering monopole coefficient $f_1(\tilde{\kappa})$ which will depend on the liquid a dead or fixed cell is suspended in. Our observations, where the vast majority of fixed and dead cells was located in the pressure node even at high iodixanol concentrations, can thus be explained by the density modified medium penetrating the compromised cell membrane, which alters the acousto-mechanical properties of the cells (Fig. 6).

We have used viable and dead as a cell state case to demonstrate acoustic binary separation based on acousto-mechanical properties. However, other factors might also influence the mechanical phenotype of cells. One such factor is the cell cycle which has shown to influence mechanical
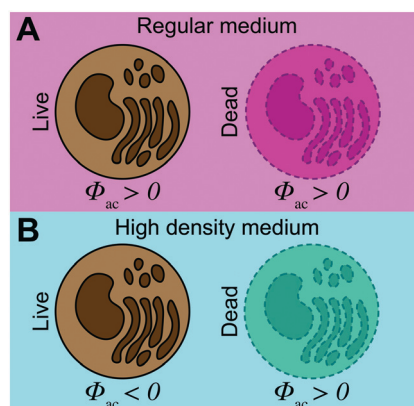
properties of HL60 cells.[22] Mechanical property changes has also been observed in rat endothelial cells under hypoxic condition[26] and the difference in mechanical phenotype in cancer cells compared to normal cells has been reported extensively.[27,28] Whether these mechanical differences between cell states are large enough for effective separation remains to be seen, but it might be part of the reason why mechanical properties are distributed in a cell population and should be considered in acoustofluidic applications.

Spatial acoustic separation of viable and dead cells using a density modified medium is promising as it enables binary sorting of the two states. Current strategies to enrich the viable population in cell cultures are based on either low speed centrifugation, fluorescence-activated cell sorting (FACS) or magnetic-activated cell sorting (MACS) which require labeling and might affect cell viability and function.[29] Yang *et al.* showed the first successful acoustophoretic separation of viable MCF-7 breast cancer cells and MCF-7 cells dead through osmotic chock.[30] They reported a slight cell size decrease in the dead population and inferred that the cell volume dependent acoustic radiation force drove the viable cells faster into the pressure node to then be collected in the center outlet of a flow splitter. Zalis *et al.* used a similar time-of-flight technique but added a pre-alignment channel and studied the separation efficacy of viable and dead MCF-7, mouse neuroblastoma N2a and human embryonic stem cells (hESCs).[31] Cell death was induced in several different ways (osmotic shock, starvation, DMSO exposure and staurosporine treatment) and they could separate viable and dead cells with high efficacy depending on condition and balance between flowrate and acoustic energy density. They observed a large cell size overlap between the dead and viable population and suggested that cell death dependent changes in acousto-mechanical properties might be responsible for the acoustic contrast factor decrease which allowed acoustophoretic time-of-flight separation. Our results substantiate this claim, but suggests a novel route for separation of dead and viable cells. When dead and living cells are relocated to the pressure node and anti-node, due to the acoustic contrast factor sign difference, there is a possibility for efficient binary separation which is less sensitive to the balance between acoustic energy density E_{ac} and flow rate in the channel.[32] While the acoustic force magnitudes acting on viable and dead cells suspended in iodixanol solutions has not been within the scope of this study, it should be noted that the dynamic viscosity increases with iodixanol concentration (approximately by a factor 2 in 30% v/v compared to 0%)[18] which affects cell displacement velocities in tandem with changes in acoustic contrast factor. Even though binary separations are efficient, optimized acoustophoresis systems are still necessary to get high separation efficacy and throughput using our method. A similar method using an acousto-mechanically modified medium to change the acoustic contrast factor has also been used to spatially separate polymer beads with different mechanical properties,[33] demonstrating the general

advantages of binary separation. We also think that the spatial separation between living and dead cells might be valuable in *e.g.* killing assays where fluorescent dyes are not a feasible option.

The ratio of living K562 and MCF-7 cells in the pressure node, anti-node and intermediate zones at different iodixanol concentration also allowed us to approximate the effective acoustic impedance Z_{cell} of viable K562 and MCF-7 cells. For the iodixanol concentration $c_{Iodixanol}$ where the acoustic contrast factor of the viable K562 and MCF-7 cells is zero, $\Phi_{ac}(\tilde{\kappa}, \tilde{\rho}) = 0$, we can approximate the acoustic impedance Z_{cell} to be equal to the acoustic impedance of the density modified medium, Z_{medium}, as outlined by Augustsson *et al.*[18] This approximation was shown to induce a maximum error of ≈1.8% for all possible combinations of reasonable cell densities and compressibilities. By assuming that the K562 and MCF-7 acousto-mechanical properties were inhomogeneous and normally distributed within the cell populations, we found that the acoustic impedance of K562 cells was Z_{K562} = 1.68 ± 0.014 MPa s m^{-1} (mean ± standard deviation) and Z_{MCF-7} = 1.67 ± 0.012 MPa s m^{-1} for MCF-7 cells. The K562 result is in good agreement with the acoustic impedance of mouse B cell line BA-F3 (1.66 MPa s m^{-1} to 1.70 MPa s m^{-1} corresponding to the 5th to 95th percentile).[18] In studies where the cell density is not taken from literature, the acoustic impedance of MCF-7 cells have been reported to be about 1.64 MPa s m^{-1} (ref. 18) and 1.68 MPa s m^{-1} (ref. 21) which is in fairly good agreement with our measurement. It should be noted that we observed some influence of acoustic streaming on cells with zero acoustic contrast factor. The acoustic streaming in combination with

Fig. 6 The compromised membrane of dead cells allows the surrounding liquid to enter the cell and change the acousto-mechanical properties. The acoustic contrast factor Φ_{ac} of a cell depends on the acousto-mechanical difference between surrounding fluid and the cell and decides whether a cell is driven to pressure node or anti-node. In media regularly used in acoustofluidic applications, both viable and dead cells have a positive contrast factor (A). When the medium density is increased, the acoustic contrast factor of viable cells changes sign, while the surrounding fluid is internalized in the dead cell through the compromised cell membrane, altering the acousto-mechanical properties and provides a positive acoustic contrast factor (B).

buoyancy in high iodixanol concentration could drive zero contrast cells with a flow towards the pressure anti-node. The anti-node directed flow could therefore introduce a systematic overestimation of the cell percentage trapped in the pressure anti-node and thus introduce a slight overestimation of the acoustic impedance. To overcome this issue, acoustic streaming suppressing strategies like channel geometry optimization should be utilized.[34] But even with the acoustic streaming caution, these results shows the potential for the methodology presented in this paper to determine effective acoustic impedance of a cell population and may be complementary to the iso-acoustic focusing platform developed by Augustsson *et al.* as it does not require a stable concentration gradient of density medium.

Cell death induced by starvation and osmotic shock did not to a large degree influence the separation efficacy compared to using fixed cells but it should be noted that the trapping velocity was lower for starvation and osmotic shock treated cells compared to fixed cells in 30% v/v iodixanol. The observed differences in separation efficacy between the cell lines tested in this study also imply that death condition and cell type might give varying results.

Conclusion

To conclude this study, we have shown that viable and dead K562, MCF-7 and A498 cells suspended in a density modified medium can be binary separated using ultrasonic standing waves in a straight microchannel due to the compromised cell membrane of dead cells. This shows that the influence of cell state on the acousto-mechanical properties is important to consider in acoustofluidic applications but can be advantageously used in separation applications. The binary separation method, based on the acoustic contrast factor, shown in this study is insensitive to cell size and to a lesser extent the balance between flow rate and acoustic energy density in a microfluidic channel compared to acoustophoretic time-of-flight methods. These factors mean that acoustophoresis-based sorting of live from dead cells using our proposed method has great potential for simple and robust operation.

Conflicts of interest

The authors declare no conflict of interest.

Acknowledgements

References

1   L. R. Volpatti and A. K. Yetisen, *Trends Biotechnol.*, 2014, **32**, 347–350.

2   H. Bruus, J. Dual, J. Hawkes, M. Hill, T. Laurell, J. Nilsson, S. Radel, S. Sadhal and M. Wiklund, *Lab Chip*, 2011, **11**, 3579–3580.

3   I. Iranmanesh, H. Ramachandraiah, A. Russom and M. Wiklund, *RSC Adv.*, 2015, **5**, 74304–74311.

4   P. Augustsson and T. Laurell, *Lab Chip*, 2012, **12**, 1742–1752.

5   M. Antfolk and T. Laurell, *Anal. Chim. Acta*, 2017, **965**, 9–35.

6   D. Bazou, W. T. Coakley, A. J. Hayes and S. K. Jackson, *Toxicol. In Vitro*, 2008, **22**, 1321–1331.

7   S. Oberti, A. Neild and J. Dual, *J. Acoust. Soc. Am.*, 2007, **121**, 778–785.

8   N. Garg, T. M. Westerhof, V. Liu, R. Liu, E. L. Nelson and A. P. Lee, *Microsyst. Nanoeng.*, 2018, **4**, 17085.

9   Y. Kurashina, K. Takemura and J. Friend, *Lab Chip*, 2017, **17**, 876–886.

10   A. Lenshof and T. Laurell, *Chem. Soc. Rev.*, 2010, **39**, 1203–1217.

11   O. Manneberg, S. Melker Hagsater, J. Svennebring, H. M. Hertz, J. P. Kutter, H. Bruus and M. Wiklund, *Ultrasonics*, 2009, **49**, 112–119.

12   U. S. Jonnalagadda, M. Hill, W. Messaoudi, R. B. Cook, R. O. C. Oreffo, P. Glynne-Jones and R. S. Tare, *Lab Chip*, 2018, **18**, 473–485.

13   K. Olofsson, V. Carannante, M. Ohlin, T. Frisk, K. Kushiro, M. Takai, A. Lundqvist, B. Onfelt and M. Wiklund, *Lab Chip*, 2018, **18**, 2466–2476.

14   H. Bruus, *Lab Chip*, 2012, **12**, 1014–1021.

15   M. Ohlin, I. Iranmanesh, A. E. Christakou and M. Wiklund, *Lab Chip*, 2015, **15**, 3341–3349.

16   J. Hultstrom, O. Manneberg, K. Dopf, H. M. Hertz, H. Brismar and M. Wiklund, *Ultrasound Med. Biol.*, 2007, **33**, 145–151.

17   M. A. Faridi, H. Ramachandraiah, I. Iranmanesh, D. Grishenkov, M. Wiklund and A. Russom, *Biomed. Microdevices*, 2017, **19**, 23.

18   P. Augustsson, J. T. Karlsen, H. W. Su, H. Bruus and J. Voldman, *Nat. Commun.*, 2016, **7**, 11556.

19   E. Strohm, G. J. Czarnota and M. C. Kolios, *IEEE Transactions on Ultrasonics, Ferroelectrics, and Frequency Control*, 2010, vol. 57, pp. 2293–2304.

20   E. C. Weiss, P. Anastasiadis, G. Pilarczyk, R. M. Lemor and P. V. Zinin, *IEEE Transactions on Ultrasonics, Ferroelectrics, and Frequency Control*, 2007, vol. 54, pp. 2257–2271.

21   K. W. Cushing, F. Garofalo, C. Magnusson, L. Ekblad, H. Bruus and T. Laurell, *Anal. Chem.*, 2017, **89**, 8917–8923.

22   O. Otto, P. Rosendahl, A. Mietke, S. Golfier, C. Herold, D. Klaue, S. Girardo, S. Pagliara, A. Ekpenyong, A. Jacobi, M. Wobus, N. Topfner, U. F. Keyser, J. Mansfeld, E. Fischer-Friedrich and J. Guck, *Nat. Methods*, 2015, **12**, 199–202, 194 p following 202.

23   K. A. Addae-Mensah and J. P. Wikswo, *Exp. Biol. Med.*, 2008, **233**, 792–809.

24   M. Radmacher, M. Fritz, C. M. Kacher, J. P. Cleveland and P. K. Hansma, *Biophys. J.*, 1996, **70**, 556–567.

25   H. Zhang and K. K. Liu, *J. R. Soc., Interface*, 2008, **5**, 671–690.

26 S. S. An, C. M. Pennella, A. Gonnabathula, J. Chen, N. Wang, M. Gaestel, P. M. Hassoun, J. J. Fredberg and U. S. Kayyali, *Am. J. Physiol.*, 2005, **289**, C521–C530.

27 M. Lekka, K. Pogoda, J. Gostek, O. Klymenko, S. Prauzner-Bechcicki, J. Wiltowska-Zuber, J. Jaczewska, J. Lekki and Z. Stachura, *Micron*, 2012, **43**, 1259–1266.

28 M. Prabhune, G. Belge, A. Dotzauer, J. Bullerdiek and M. Radmacher, *Micron*, 2012, **43**, 1267–1272.

29 A. P. Gee and A. G. Durett, *Cytotherapy*, 2002, **4**, 91–92.

30 A. H. Yang and H. T. Soh, *Anal. Chem.*, 2012, **84**, 10756–10762.

31 M. C. Zalis, J. F. Reyes, P. Augustsson, S. Holmqvist, L. Roybon, T. Laurell and T. Deierborg, *Integr. Biol.*, 2016, **8**, 332–340.

32 T. Laurell, F. Petersson and A. Nilsson, *Chem. Soc. Rev.*, 2007, **36**, 492–506.

33 S. Gupta, D. L. Feke and I. Manas-Zloczower, *Chem. Eng. Sci.*, 1995, **50**, 3275–3284.

34 J. S. Bach and H. Bruus, 2020, arXiv:2002.11058 [physics.flu-dyn].